Mobile dynamic passive sampling of trace organic compounds: Evaluation of sampler performance in the Danube River

Branislav Vrana [a,*], Foppe Smedes [a], Ian Allan [b], Tatsiana Rusina [a], Krzysztof Okonski [a], Klára Hilscherová [a], Jiří Novák [a], Peter Tarábek [c], Jaroslav Slobodník [d]

[a] Masaryk University, Faculty of Science, Research Centre for Toxic Compounds in the Environment (RECETOX), Kamenice 753/5, 625 00 Brno, Czech Republic
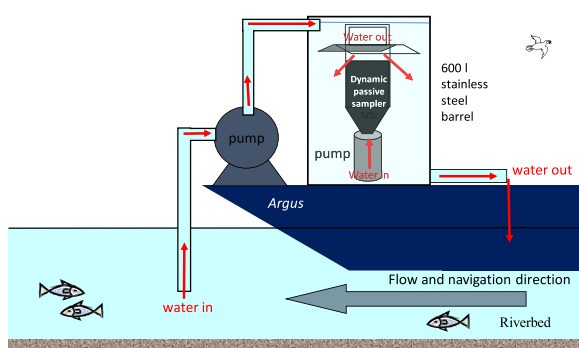[b] Norwegian Institute for Water Research, Gaustadalle'en 21, NO-0349 Oslo, Norway
[c] Water Research Institute, Nábr. arm. gen. L. Svobodu 5, 81249 Bratislava, Slovakia
[d] Environmental Institute, Okružná 784/42, 972 41 Koš, Slovakia

HIGHLIGHTS

- A dynamic passive sampling device was designed to speed up the chemical uptake
- The device was applied in the Danube river for sampling from a cruising ship
- Spatially and temporally integrated samples of dissolved compounds were obtained
- The device samples up to 5 times faster in comparison with a caged passive sampler
- Mutual comparability of three passive samplers deployed in parallel was shown

GRAPHICAL ABSTRACT

ARTICLE INFO

ABSTRACT

A "dynamic" passive sampling (DPS) device, consisting of an electrically driven large volume water pumping device coupled to a passive sampler exposure cell, was designed to enhance the sampling rate of trace organic compounds. The purpose of enhancing the sampling rate was to achieve sufficient method sensitivity, when the period available for sampling is limited to a few days. Because the uptake principle in the DPS remains the same as for conventionally-deployed passive samplers, free dissolved concentrations can be derived from the compound uptake using available passive sampler calibration parameters. This was confirmed by good agreement between aqueous concentrations of polycyclic aromatic hydrocarbons (PAHs), polychlorinated biphenyls (PCBs) and hexachlorobenzene (HCB) derived from DPS and conventional caged passive sampler. The DPS device enhanced sampling rates of compounds that are accumulated in samplers under water boundary layer control (WBL) more than five times compared with the conventionally deployed samplers. The DPS device was deployed from a ship cruising downstream the Danube River to provide temporally and spatially integrated concentrations. A DPS-deployed sampler with surface area of 400 cm^2 can reach sampling rates up to 83 L d^{-1}. The comparison of three passive samplers made of different sorbents and co-deployed in the DPS device, namely silicone rubber (SR), low density polyethylene (LDPE) and SDB-RPS Empore™ disks showed a good correlation of surface specific uptake for compounds that were sampled integratively during the entire exposure period. This provided a good basis for a cross-calibration between the samplers. The good correlation of free dissolved PAHs, PCBs and HCB

* Corresponding author at: Research Centre for Toxic Compounds in the Environment (RECETOX), Faculty of Science, Masaryk University, Kamenice 753/5, pavilon A29, 625 00 Brno, Czech Republic.
E-mail address: vrana@recetox.muni.cz (B. Vrana).

concentration estimates obtained using SR and LDPE confirmed that both samplers are suitable for the identification of concentration gradients and trends in the water column. We showed that the differences in calculated aqueous concentrations between sampler types are mainly associated with different applied uptake models.

1. Introduction

Organic compounds are often present in the water column of rivers and lakes at trace concentrations that are difficult to detect when conventional low volume spot sampling of water is applied. Despite the low concentrations, chemicals can present a significant risk to aquatic organisms and humans, and many of them are regulated in surface waters (EU, 2013, 2000). Reliable and representative monitoring is required for assessing compliance of water bodies with environmental quality standards, or for characterizing spatial and temporal contamination trends.

Among available methods, passive sampling presents a promising approach to future regulatory monitoring of trace organic compounds (Booij et al., 2016; Lohmann et al., 2012). Besides practical advantages that include passive in situ concentration and preservation of sampled compounds in sorbent materials, passive sampling provides freely dissolved compound concentrations, C_w (Vrana et al., 2005). The C_w is considered to play a key role in understanding chemical's exposure of aquatic organisms (Reichenberg and Mayer, 2006).

When conventional passive water samplers are applied, they must be deployed for several weeks or months, because their ambient sampling rates (R_s), representing the volume of water extracted per unit of time, are low. However, when the time period available for passive sampling is restricted, compensation by high sampling rate is needed to sample a sufficient volume of water for instrumental quantification or measuring chemical effects using bioanalytical tools.

Since R_s proportionally increase with the surface area of a sampler (Booij et al., 2007) they can be increased by using samplers in the form of large thin sheets. Furthermore, R_s increase when the water flow rate or turbulence on the sampler surface is higher (Estoppey et al., 2014; Li et al., 2010; Vermeirssen et al., 2009; Vrana and Schüürmann, 2002). Faster flow conditions cause a thinner water boundary layer (WBL) and lead to lower resistance to mass transfer (Levich, 1962). This is because the mass transfer of hydrophobic compounds is typically controlled by their diffusion through the WBL (Rusina et al., 2007). Flow turbulence can be increased by positioning samplers in a natural or artificially created current, by shaking, rotating or vibrating them during exposure in water (Qin et al., 2009). Allan et al. (2011) have shown increased R_s by towing samplers fastened to the end of a benthic trawl net. In general, input of some external mechanical energy is needed for increasing the water turbulence in vicinity of the samplers.

In this study, we investigated the applicability of a novel "dynamic" passive sampling device (DPS) that was developed with the aim to maximize the sampling rates of pollutants by forcing water at high flow rate along the passive sampler surface. The high flow was achieved by jetting water through a narrow flow-through sampler exposure chamber using a pump. Hereto we 1) compared the performance of DPS with conventional deployment of passive samplers in cages; 2) tested the performance of the DPS device by deployment from a moving ship in the Danube river to obtain integrated freely dissolved concentrations of pollutants in the water column over time and space; 3) compared the uptake of compounds by silicone rubber, low density polyethylene and SDB-RPS Empore™ disks samplers co-deployed inside the DPS device. The first two materials are commonly used for sampling hydrophobic compounds, whereas the latter is used also for sampling hydrophilic compounds. Finally, 4) we evaluated aqueous concentrations of atrazine derived from DPS in relation to those from spot water sampling.

2. Materials and methods

2.1. Passive samplers

Three types of passive samplers were applied: two partitioning samplers, SR and LDPE sheets and one adsorption sampler based on styrene-divinylbenzene solid phase extraction disks, SDB-RPS Empore™ disks (ED). AlteSil™ translucent SR sheets 0.5 mm thick (Altec, UK) were cut into samplers with a size of 14×28 cm (392 cm^2, 23 g), Soxhlet extracted in ethylacetate for 72 h and spiked according to the procedure described in Smedes and Booij (2012) with 14 performance reference compounds (PRC: D_{10}-biphenyl and 13 polychlorinated biphenyl (PCB) congeners that do not occur in technical mixtures; see Supplementary information (Section 1). LDPE (Brentwood Plastics Inc, St. Louis, USA) strips of 4×28 cm (112 cm^2) and 70 μm thickness were spiked with the 6 perdeuterated polycyclic aromatic hydrocarbons (PAHs) as PRC (S1.2. An ED sampler consisted of ten 47 mm in diameter Empore® SDB-RPS disks (Sigma Aldrich, Czech Republic), with a total mass of approximately 3.2 g and 173 cm^2 surface area. Before exposure, ED samplers were cleaned in acetone, isopropanol, methanol and milliQ water, in which they were stored at 4 °C. ED samplers were not spiked with PRC. Note that the stated total sampler surface area was nominal, while in practice 80% had contact with water and ~20% was covered by the grid holding them in place.

2.2. Water sampling

2.2.1. Sampling device

The DPS device consists of a rectangular stainless-steel plate chamber with an open grid on both sides. (Figs. S1 and S2; Supplementary information). The different samplers were placed on the grid (Fig. 1) and covered by the lids. One end of the chamber was connected to a submersible pump (approximately 9 m^3 h^{-1}) that forced water at high flow velocity (1–2 m s^{-1}) through the chamber while being immersed in the water. Temperature was monitored by a submersible logger (Hobo Pendant, Onset, Germany) attached to the DPS device. The cruising speed of the ship did not allow immersion of the DPS device directly in the river water and therefore it was immersed in a flow-through system using a 600 L stainless steel tank positioned onboard the ship (Fig. S3, Supplementary information). The water was pumped through the tank at a rate of about 3 m^3 h^{-1} from a stainless-steel inlet tube positioned in front of the ship about 0.5 m below the water surface (Fig. S4, Supplementary information). Sampling by the DPS device on the ship did not decrease the exposure concentration in the tank as its R_s of <100 L d^{-1} was negligibly low in comparison with the 72,000 L d^{-1} flow through the tank.

2.2.2. Deployment and retrieval

Samplers were always mounted in the DPS device just before exposure and retrieved immediately afterwards. Upon recovery, the surfaces of SR and LDPE samplers were cleaned using a pre-cleaned scourer and local river water. The surface of the ED samplers did not permit cleaning. Recovered samplers were placed back into their storage containers, stored at 4 °C on board of the ship, transported to the laboratory within a week, and stored at −20 °C until further processing. To estimate any contaminant uptake not associated with water exposure, field blank samplers were exposed to air in a stainless-steel tray during sampler's mounting and retrieval.

Fig. 1. Co-deployed AlteSil™ silicone rubber (SR sampler), SDB-RPS Empore disks (ED sampler) and LDPE stripes (LDPE sampler) in a DPS device. The arrows show the direction of water streaming through the exposure chamber.

2.2.3. Sampling campaign

The sampling campaign was performed in August and September 2013 as part of the Joint Danube Survey 3 (JDS 3) by the expedition ship Argus (Liška et al., 2015). Passive sampling of organic compounds was performed over eight stretches of the Danube using the DPS device on board of the ship (Fig. 2) in an approach similar to a FerryBox concept (Petersen, 2014) and the mobile continuous flow system (Petersen et al., 2016). Each individual water sampling period covered approximately 5 days, the time the ship moved downstream along a defined stretch. Note that the DPS was only in operation when cruising or anchored in the river. The device was always switched off before the ship entered harbours and switched on again when the cruise resumed. Consequently, actual sampling periods were about two days per stretch (Table 1).

During the period the ship sampled stretches 1 and 2, two subsequent stationary samplings of 4 and 5 days each were conducted at a site located 1852 km distant from the Danube river mouth. They were performed from shore using a DPS device immersed in river water at the depth of approximately 1 m (Table 1 and Fig. 2). In addition, a SR and an ED sampler were passively deployed for 43 days (Table 1) in a perforated stainless steel cage (caged sampler). Unfortunately, LDPE sampler deployed in a cage was lost during sample transport.

Spot samples of surface water in bottles were also collected from the expedition ship at 63 sites in the 8 Danube stretches covered by passive sampling. The time of spot sample collection within each river stretch was always within the time period of passive sampler deployment (Table 1). A range of priority substances was analysed in whole water samples by several expert laboratories (Deutsch and Sengl, 2015). The results were reported to the International Commission for the Protection of the Danube river and are accessible in a database (ICPDR International Commission for the Protection of the Danube River, n.d.).

2.3. Sampler analysis

2.3.1. Silicone rubber (SR) sheets

Exposed, field blank, and control SR samplers, were spiked with SR recovery internal standards (SR RIS; Section 1 in Supplementary

information) and Soxhlet extracted for 8 h with methanol. The extract was concentrated by Kuderna-Danish (KD) apparatus to 4 mL, dried over anhydrous Na_2SO_4, and further concentrated to 2 mL under a gentle nitrogen flow. A 20% aliquot was used for analysis of alkyl phenols and polar compounds by LC/MS methods. Twenty mL hexane was added to the remaining extract, and methanol was azeotropically removed by KD concentration. An aliquot representing 20% of the total extract in hexane was further cleaned-up over a silica gel column by elution with diethyl ether/acetone, and used for analysis of PAHs and other target groups of compounds. The remaining 60% was purified using activated silica gel modified with sulphuric acid for the analysis of OCPs, PCBs, PRCs and other halogenated compounds. After addition of syringe internal standards (IS) and volume reduction both extracts were analysed by GC–MS/MS (Section 2 in Supplementary information).

2.3.2. Low density polyethylene (LDPE) sheets

All LDPE samplers, including field controls, were extracted twice by soaking overnight with *n*-pentane (100 mL) after addition of LDPE RIS (Section 1 in Supplementary information). The volume of pentane was reduced to 2 mL by a gentle stream of nitrogen at room temperature. Extracts were first split into two equal fractions by volume. One fraction received a general clean-up using gel permeation chromatography (GPC). This post GPC sample was again split into two equal fractions by volume; the first of these fractions was reduced in volume using nitrogen and analysed for PAHs; the second one received treatment with 2×1 mL concentrated sulphuric acid, was reduced in volume, and analysed for PCBs and OCPs. Details of the procedure and instrumental analysis are described in (Allan et al., 2013).

2.3.3. Empore disks

All ED samplers for chemical analysis were spiked with ED RIS (Section 1 in Supplementary information). Samplers were then freeze dried for 24 h in the original storage and transport containers and extracted three times by slow shaking (12 h) at room temperature with 70 mL acetone. The volume of combined extracts was reduced by vacuum rotary evaporation and, after removal of particles by filtration through a layer of anhydrous Na_2SO_4, further reduced in volume to

Fig. 2. Map of the Danube river stretches and the stationary station (the red circle) passively sampled in August and September 2013. Details of sampling in individual stretches are given in Table 1. (For interpretation of the references to colour in this figure legend, the reader is referred to the web version of this article.)

approximately 1 mL. Solvent transfer to methanol was performed by addition of methanol (20 mL) and subsequent volume reduction to 2 mL by a nitrogen flow. Aliquots were used for various instrumental analytical methods. An aliquot representing 10% of the total extract was further azeotropically solvent exchanged by KD to hexane for analysis of PAHs.

2.4. Data analysis

2.4.1. Sampling rate calculation

The compound sampling rate of a sampler made of polymer x, $R_{s,x}$, represents the volume of water extracted per unit of time. Compound diffuses to the sampler through the WBL and the polymer membrane comprising the sampler (Booij et al., 2007), and is finally sorbed. The overall resistance to mass transfer, i.e. the reciprocal value of the overall mass transfer coefficient, $k_{o,x}$, can be expressed as the sum of the transport resistances in WBL and polymer:

$$\frac{1}{k_{o,x}} = \frac{1}{k_w} + \frac{1}{k_x K_{x,w}} \tag{1}$$

where k_w and k_x are the mass transfer coefficients in the WBL and the membrane (made of polymer x), respectively, and $K_{x,w}$ is the polymer x–water partition coefficient. The transport resistances for a compound through WBL and membrane, are inversely proportional to the diffusion coefficients, D_w and D_x, and proportional to their thicknesses δ_w and δ_x,

Table 1
Meta data for sampling from the Argus ship at the various Danube river stretches and a stationary station in August and September 2013.

Stretch	Stretch start and end	River km[a]	Dates of cruise and sampler deployment	Mean water temperature [°C]	Exposure time [d]
S1	Passau-Bratislava	2203–1852	17.8.–22.8.	21.3	2.0
Stationary deployment; DPSa[b]	*Downstream Bratislava*	*1852*	*19.8.-23.8.*	*21.3*	*4.0*
Stationary deployment; DPSb[b]	*Downstream Bratislava*	*1852*	*23.8.-28.8.*	*21.3*	*5.0*
Stationary deployment; Caged sampler	*Downstream Bratislava*	*1852*	*28.8.-10.10.*	*20.0*	*43*
S2	Bratislava-Budapest	1852–1632	22.8.-26.8.	22.0	1.2
S3	Budapest-Vukovar	1648–1297	26.8.-2.9.	21.9	1.7
S4	Vukovar-Belgrade	1297–1154	2.9.-6.9.	22.8	1.6
S5	Belgrade-Turnu-Severin	1154–930	6.9.-10.9.	22.1	2.0
S6	Turnu-Severin-Ruse	930–495	11.9.-17.9.	21.9	2.0
S7	Ruse-Braila	495–170	17.9.-21.9.	19.2	1.4
S8	Braila-Tulcea	170–71	21.9.-26.9.	18.7	1.3

[a] The distance from the river mouth.
[b] The two subsequent stationary deployments of a DPS are labeled as DPSa and DPSb, respectively.

respectively. Compounds, however, do not only simply diffuse through the membrane but are also accumulated in the membrane. The diffusion pathlength in the membrane can be approximated using $0.5 \times \delta_x$ (Salaun and Buffle, 2004; Ter Laak et al., 2008). Consequently, Eq. (1) transforms to:

$$\frac{1}{k_{o,x}} = \frac{\delta_w}{D_w} + \frac{0.5\,\delta_x}{K_{x,w}\,D_x} \qquad (2)$$

Finally, the product of the mass transfer coefficient and sampler-surface area in contact with water (A_x) equals the sampling rates $R_{s,x}$ ($L\,d^{-1}$) as

$$R_{s,x} = k_{o,x}A_x = \frac{A_x}{\dfrac{1}{k_w} + \dfrac{0.5\,\delta_x}{K_{x,w}D_x}} \qquad (3)$$

Membrane-controlled mass transfer has to be considered especially for compounds with low $K_{x,w}$, since the transport resistance is inversely proportional to the $K_{x,w}$, and, as a result, for less hydrophobic compounds the transport resistance in polymer often controls the uptake rate (Booij et al., 2007). In case the transport resistance in polymer is negligible, Eq. (3) reduces to.

$$R_{s,x} = k_w A_x = \frac{D_w}{\delta_w}A_x \qquad (4)$$

The latter term follows from Eq. (2) showing R_s's dependence on the turbulence represented by δ_w and compound's specific D_w. These two factors were captured in a model (Rusina et al., 2010b):

$$R_{s,x} = A_x k_w = A_x B M^{-0.47} \qquad (5)$$

where M is the molar mass ($g\,mol^{-1}$) inserting effect of D_w, and B an exposure specific proportionality factor representing the flow conditions and containing the factor for unit conversion.

For SR and LDPE samplers, in–situ sampling rates were estimated using retained PRC fractions $f(PRC)$ as the ratio between PRC concentrations in the sampler after exposure time t and at $t = 0$. The modeled retained fraction is a function of exposure time t and $K_{x,w}$ following:

$$f(PRC) = \exp\left(-\frac{R_{s,x}t}{K_{x,w}m_x}\right) \qquad (6)$$

where m_x is the sampler mass. After inserting Eq. (5) into Eq. (6), modeled $f(PRC)$ are fitted to measured $f(PRC)$ using nonlinear regression with B as adjustable parameter (Booij and Smedes, 2010). Compound specific $R_{s,x}$ were then calculated using Eq. (5) as shown for SR in Fig. S5 in Supplementary information.

When also membrane-controlled mass transfer has to be considered, Eq. (3) can be inserted in Eq. (6) and $R_{s,x}$ calculated applying a similar fitting with k_w as adjustable parameter.

Because the ED sampler is an adsorption-based sampler, desorption kinetics are generally not isokinetic with the uptake. Therefore, calculation of sampling rates for the ED sampler from PRC elimination cannot be applied (Shaw et al., 2009). For compounds under investigation with assumed integrative uptake the $R_{s,ED}$ of ED samplers were derived from a correlation of uptake of PAHs and nonylphenol by ED and SR samplers as shown in the Results section.

2.4.2. Models for calculating sampling rates in LDPE sheets

Three approaches were tested to estimate sampling rates for LDPE sheets.

'A', we assumed equality of WBL-controlled mass transfer coefficients in SR and LDPE samplers, and therefore mass transfer coefficients derived for SR samplers were applied to the LDPE samplers. $R_{s,LPDE}$ values were then calculated using Eq. (3) applying the $k_w = BM^{-0.47}$ derived from PRC dissipation from SR (Eq. (5)). The required D_{LDPE} and $K_{LDPE,w}$ values were taken from (Rusina et al., 2010a) and (Smedes et al., 2009).

'B', $R_{s,LPDE}$ was calculated from PRC dissipation using the combination of Eqs. (3) and (6) and resistances to mass transfer in both WBL and polymer were modeled as a function of compound hydrophobicity using the model proposed by (Booij et al., 2003). Details of the model are given in Section 4 in Supplementary information.

'C', WBL controlled R_s was calculated from dissipation data of d_{12}-CHR and d_{12}-BeP using the combination of Eqs. (5) and (6). Only two PRCs could be included in the model, since the remaining PRCs either completely dissipated from the sampler or their release was partially controlled by the membrane. $R_{s,LPDE}$ values were then calculated using Eq. (3).

2.4.3. Estimation of free dissolved concentration in water

Uptake of analytes absorbed by the samplers follows a first-order approach to equilibrium. DEQ_x is the degree of equilibrium that the chemical attained during sampler exposure:

$$DEQ_x = \left(1 - \exp\left(-\frac{R_{s,x}t}{K_{x,w}m_x}\right)\right) \qquad (7)$$

The uptake can be considered integrative until DEQ_x reaches the value of 0.5. The required $K_{x,w}$ values of PAHs and PCBs in SR/water and LDPE/water system are available from (Smedes et al., 2009).

Aqueous concentrations $C_{w,x}$ for SR and LDPE samplers were calculated from the mass absorbed by the samplers N_x, the in situ sampling rate ($R_{s,x}$) of the chemicals and their sampler-water partition coefficients $K_{x,w}$ as described in (Booij et al., 2007):

$$C_{w,x} = \frac{N_x}{K_{x,w}\,m_x\,DEQ_x} \qquad (8)$$

Aqueous concentrations $C_{w,ED}$ for ED samplers were calculated according to (Booij et al., 2007), assuming a linear uptake mode during the entire exposure:

$$C_{w,ED} = \frac{N_x}{R_{s,ED}t} \qquad (9)$$

However, for prolonged exposure times the extracted volume is constrained by the uptake capacity of the passive sampler ($K_{ED,w} \times m_{ED}$) and in such case, Eq. (8) should be applied, that considers equilibration of sampler with the sampled water. Unfortunately, published $K_{x,w}$ values for ED are rare and currently not available for PAHs and alkylphenols.

3. Results and discussion

3.1. Performance of the DPS device

3.1.1. Comparison of caged sampler and DPS

The $C_{w,SR}$ of PAHs, PCBs and HCB were calculated using analyte amounts accumulated in SR and the $R_{s,SR}$ obtained as described in Section 2.4. The $C_{w,SR}$ for stationary caged samplers and stationary DPS devices downstream Bratislava agreed very well (Fig. 3, left graph), with a median ratio of 0.93 and 0.83 for individual PAHs and PCBs, respectively. Similarly, a reasonably good median $C_{w,SR}$ ratio was obtained for individual PAHs and PCBs from caged samplers and mobile passive samplers in the stretch between Passau-Bratislava (Fig. 3, right graph), namely 0.74 and 0.61, respectively. In both cases the largest differences were observed for PAHs with two and three aromatic rings, which were present in water at highest concentrations.

The good $C_{w,SR}$ agreement was observed despite different sampling rates and water volumes sampled by the caged and DPS device mounted samplers. From our previous experience with passive sampling (Vrana
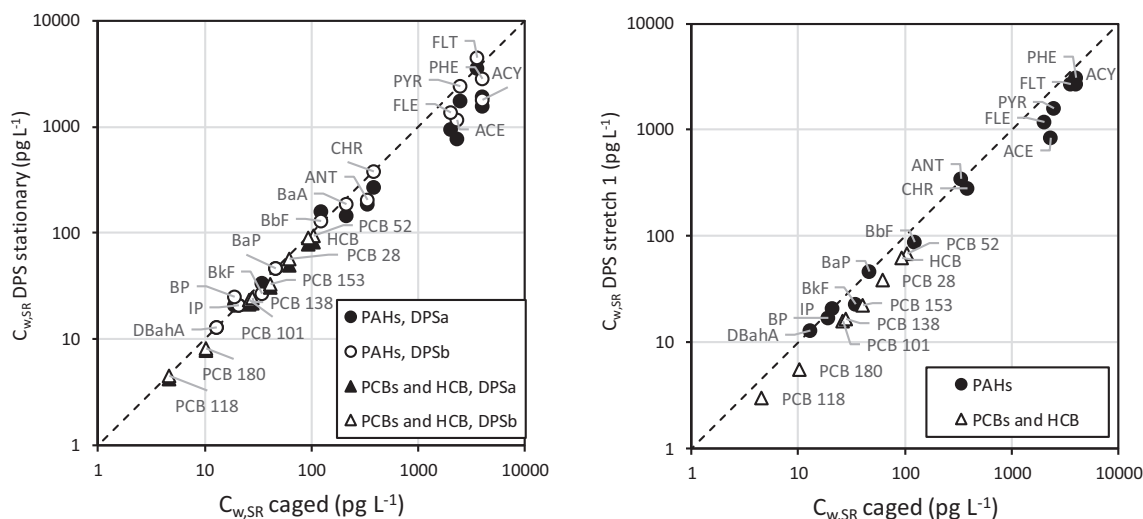
Fig. 3. Comparison of concentrations in water $C_{w,SR}$ (pg L^{-1}) of selected PAHs (circles), PCBs and HCB (triangles) derived from uptake in caged SR passive samplers at a stationary site (x-axis data) with data from stationary DPS (left graph) and mobile DPS (right graph). The dashed lines represent equality of the plotted variables. Details of exposures are given in Table 1. Compound abbreviations are explained in Supplementary information, Table S1.

et al., 2014) and based on reported PCB concentrations bound to suspended particulate matter (Umlauf et al., 2015), concentrations of PAHs and PCBs in the Danube water were not expected to fluctuate dramatically. Assuming low temporal variation of $C_{w,SR}$, observed differences in uptake are mainly related to the chemical's DEQ_{SR} (Eq. (7)) attained in different samplers. For selected PAHs, PCBs and HCB, Fig. S6 in Supplementary information shows that when uptake during the different samplings are inter-connected by a line, the curves resemble linear relation with DEQ_{SR} up to 0.5 and an exponential rise to a maximum as DEQ_{SR} approaches 1.

3.1.2. Evaluation of DPS sampling rates during the Danube cruise

The $^{300}R_{s,SR}$ (R_s for a compound with molar mass $M = 300$ g mol^{-1}) took the value of 83, 62 and 53 L d^{-1} for the mobile DPS along stretch 1, and the two stationary DPS exposures, respectively (Fig. 4). Meanwhile, $^{300}R_{s,SR}$ was only 16 L d^{-1} for the caged sampler, although it had the same surface area A_x and was deployed in a rapid river current with a flow velocity of approximately 1 m s^{-1}. Even much lower sampling

rates are envisaged with caged samplers in stagnant waters. Thus, the DPS device can increase R_s by >5-fold in comparison with the caged samplers. This is extremely useful when ultra trace compounds need to be enriched within a short time.

During the ship cruise $^{300}R_{s,SR}$ decreased by up to 35%, from 83 to 54 L d^{-1} (Table S2; Fig. 4). Using the available data on temperature dependence of SPMD sampling rates (Vrana et al., 2014), the decrease of temperature from 23 to 19 °C is expected to result in a reduction of aqueous diffusion leading to lower mass transfer through the WBL by approximately 20%. Indeed, $^{300}R_{s,SR}$ is correlated with water temperature during the cruise ($R = 0.81$). The remaining 15% decrease in $^{300}R_{s,SR}$ may be related to the decreasing effectiveness of the pump on DPS device during continuous operation over 2 months. The lower DPS sampling rates at the stationary site can be explained by a possible negative effect of river current, reducing the suction pressure of the submersible pump in the DPS device. In contrast, the mobile DPS device was positioned in a barrel with a constant hydrostatic pressure and no other water flow than that created by the pump itself.
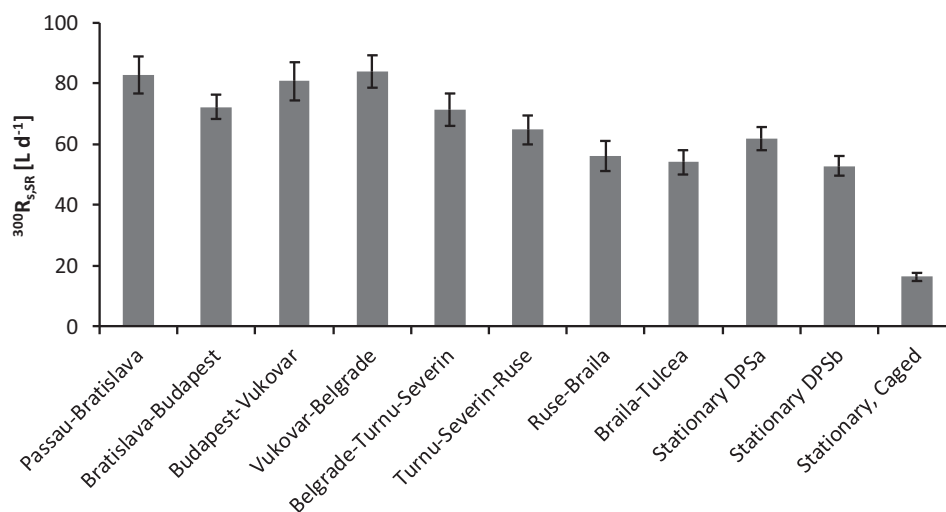

Fig. 4. Comparison of sampling rates ($^{300}R_{s,SR}$ value of a model compound with a molar mass of 300 g mol^{-1}) of SR samplers deployed in the DPS device at various stretches, one stationary station with two DPS deployments, and one caged deployment.

Table 2

Uptake parameters for compounds detected above their limit of quantification in SR and LDPE samplers. $R_{s(m)}$ is a hypothetical sampling rate in a situation when the compound uptake is fully controlled by diffusion in polymer membrane. $R_{s,x}$ shows the range of in situ sampling rates determined during exposure of samplers in the Danube River. $R_{s,LDPE}$ were calculated using method 'A' outlined in Section 2.4.2.

Compound	Abb.	Log K_{ow}	Sampler	log $K_{x,w}$ (L kg^{-1})[1]	log D_x (m^2 s^{-1})[2]	δ_x (μm)	A_x (cm^2)	$R_{s(m)}$ (L d^{-1})	$R_{s,x}$ (L d^{-1})	$k_{o,x}$ (μm s^{-1})
Phenanthrene	PHE	4.57	SR	4.11	−10.18	500	392	11,530	68–108	20–32
			LDPE	4.22	−12.45	70	112	163	17–25	18–26
Fluoranthene	FLT	5.22	SR	4.62	−10.40	500	392	22,483	64–101	19–30
			LDPE	4.93	−12.75	70	112	470	17–27	18–27
Pyrene	PYR	5.18	SR	4.68	−10.40	500	392	25,814	64–101	19–30
			LDPE	5.10	−12.82	70	112	527	17–27	18–27
Chrysene	CHR	5.86	SR	5.25	−10.61	500	392	59,137	60–94	18–28
			LDPE	5.78	−13.28	70	112	874	17–26	17–27
PCB 28	PCB 28	5.67	SR	5.53	−10.13	500	392	340,298	57–90	17–27
			LDPE	5.40	−12.51	70	112	2146	16–25	17–26
Hexachlorobenzene	HCB	5.50	SR	5.05	−10.12	500	392	115,308	54–86	16–25
			LDPE	5.43	−12.68	70	112	1555	15–24	16–25

[1] Values of $K_{SR,w}$ and $K_{LDPE,w}$ were taken from (Smedes et al., 2009).
[2] Values of log D_x were taken from Rusina et al. (2010a).

To verify that the uptake was WBL controlled for the entire hydrophobicity range under deployment conditions in SR and LDPE samplers, the overall sampling rate $R_{s,x}$ should be much lower than the estimated sampling rate $R_{s(m)}$ if controlled by diffusion in polymer:

$$R_{s,x} << R_{s(m)} \approx \frac{D_x K_{x,w} \rho_x A_x}{0.5\delta_x} \qquad (10)$$

where ρ_x is the density of polymer. The calculation confirmed that in both samplers and in all exposures, mass transfer was dominantly WBL controlled for all compounds (Table 2).

3.2. Comparing uptake by three co-deployed passive samplers

Mutual comparison of compound uptake in the three co-deployed samplers is useful to reveal similarities or differences in mass transfer mechanisms and partition equilibria of compounds in different samplers. The sampler inter-comparability is based on a rationale of the same underlying principles for the compound mass transfer from water to SR, LDPE and ED passive samplers. Moreover, in the DPS devices all three sampler types were one sided exposed in the same arrangement as flat sheets or disks that were flushed with river water at a constant flow velocity (Fig. 1). However, the samplers differed in surface area, thickness and shape of sheets/disks, the quality and mass of polymer or sorbent material applied.

Since in the integrative uptake phase the amount of a compound accumulated in the sampler $N_{t,x}$ is proportional to the sampling rate ($N_{t,x} = C_{w,x} \times R_{s,x} \times t$) and that in turn is proportional to sampler surface area A_x (Kees Booij et al., 2007), consequently, the surface specific compound uptakes $N_{t,x}/A_x$ (ng cm^{-2}) are expected to be mutually comparable.

3.2.1. Comparison of surface specific uptake in SR and LDPE

Among the measured compounds, quantifiable concentrations were found in all exposed SR and LDPE samplers only for six compounds: phenanthrene (PHE), fluoranthene (FLT), pyrene (PYR), chrysene (CHR), hexachlorobenzene (HCB) and PCB 28. The remaining PCBs and PAHs were quantifiable in SR, but mostly below the LOQ in LDPE samplers. The lower uptake to LDPE in comparison to SR is related to its 3.5-times lower surface area and its 30-times lower mass, which results in lower sampling rates and lower uptake capacity ($K_{x,w} \times m_x$), respectively (Booij et al., 2017).

The $N_{t,x}/A_x$ in LDPE and SR passive samplers and their ratios are shown in Figs. S7 and S8 in Supplementary information, respectively. Except for CHR, the $N_{t,SR}/A_{SR}$ was higher than $N_{t,LDPE}/A_{LDPE}$. The highest deviations of the ratio from unity were observed for PHE (5.1 to 14.2), FLT (1.5 to 4.6), and PYR (1.1 to 2.6). For CHR the ratio ranged from

0.5 to 1.1. Ratio values 1.1 to 1.8 and 1.2 to 2.4 were observed for HCB and PCB 28, respectively. The observed differences in $N_{t,x}/A_x$ can be caused either by a different degree of partitioning equilibrium reached in LDPE and SR samplers (Fig. S9 in Supplementary information) or by a difference in the mass transfer controlling resistance (WBL vs. membrane controlled uptake).

Since integrative uptake to SR was observed for all compounds (i.e. $DEQ_{SR} < 0.5$ in most cases), the ratio of $N_{t,x}/A_x$ in SR and LDPE was drawn against the DEQ_{LDPE}, where curvilinear uptake phase of compounds was reached in many exposures (Fig. 5). The graph shows that for all compounds the $N_{t,x}/A_x$ ratio increases with the increasing DEQ_{LDPE}, but remains close to unity (within approximately a factor of two) where the sampling is integrative in both samplers, i.e. when $DEQ_{LDPE} < 0.5$. Higher $N_{t,x}/A_x$ in SR than in LDPE of PHE and FLT uptake is related to a longer integrative sampling in SR compared to LDPE.

3.2.2. Comparison of surface specific uptake in SR and ED

The surface specific uptake ($N_{t,x}/A_x$) in ED and SR was compared for PAHs and nonylphenol, since they were well measurable in both
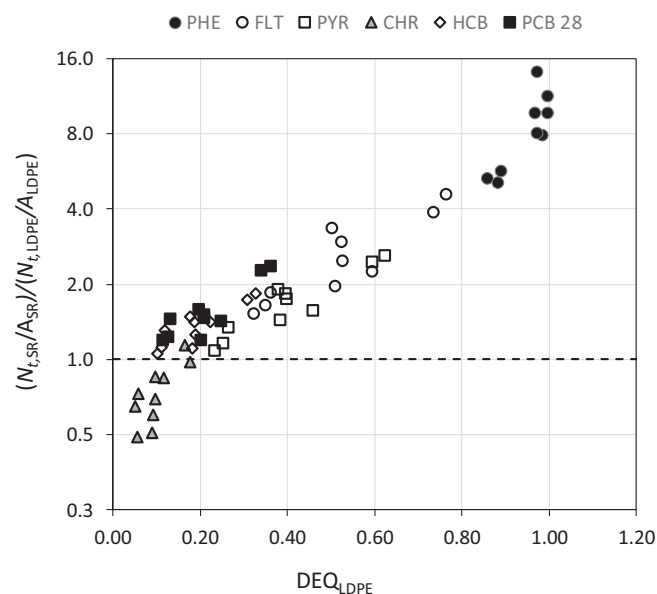

Fig. 5. Ratio of surface specific uptake of selected PAHs, PCB 28 and HCB in SR and LDPE samplers as related to the degree of equilibrium with water reached by the LDPE sampler (DEQ_{LDPE}). The dashed line represents the ratio equal to unity. DEQ_{LDPE} was calculated using method 'A' outlined in Section 2.4.2.

samplers. In SR, integrative uptake was observed for compounds with log $K_{SR,w} > 4.5$ during the entire exposure period in all exposed samplers; i.e. for 10 PAHs with more than three aromatic rings in their molecule, as well as for 4-nonylphenol (Fig. S10 in Supplementary information). The comparison was performed for these compounds. The $N_{t,x}/A_x$ in SR and ED samplers showed a very good correlation for the selected substances (Fig. 6). The comparison of surface specific uptake in individual sampler exposures is shown in detail in Supplementary information (Fig. S11).

A ratio $F_{ED/SR}$ of surface specific compound uptake in both samplers was calculated as:

$$F_{ED/SR} = \frac{N_{t,ED}/A_{ED}}{N_{t,SR}/A_{SR}} \tag{11}$$

The $F_{ED/SR}$ for the selected substances was close to unity and the overall median value was 0.83. The median value of $F_{ED/SR}$ for individual substances ranged from 0.7 to 1.2 for benzo[e]pyrene and benz[a]anthracene, respectively (Fig. S12, Supplementary information). The highest $F_{ED/SR}$ variability was mainly observed for compounds with the concentrations in passive samplers close to limit of quantification. The $F_{ED/SR}$ did not show any significant trend with the concentration level in samplers or with $K_{SR,w}$ values of test compounds (Fig. S13, Supplementary information). Thus, we assume that the observed variability of $F_{ED/SR}$ for different compounds and different exposures is caused mainly by analytical variability. In conclusion, the good correlation of $N_{t,x}/A_x$ in various compared samplers for compounds that are sampled integratively provides an excellent basis for a robust cross-calibration between the samplers.

3.2.3. Comparison of C_w derived from uptake to SR and LDPE

In the next step we evaluated the agreement of $C_{w,x}$ values derived from compound uptake in SR and LDPE samplers. Since comparable surface specific uptake ($N_{t,x}/A_x$) in the two samplers was observed for chemicals under WBL control, the differences in calculated $C_{w,x}$ values for those chemicals should be mainly attributed to the differences in the models applied for $C_{w,x}$ calculation.

$C_{w,SR}$ were calculated using the approach outlined in Section 2.4.1 and 2.4.3 and three different models (2.4.2) were applied for interpretation of uptake data from LDPE sampler. $C_{w,LDPE}$ data obtained using the three models were then checked for consistency with $C_{w,SR}$ data (Fig. S14, Supplementary information). For all compounds with exception of PHE and FLT, a very good correlation (correlation coefficient R between 0.74 and 0.96) was found between $C_{w,x}$ values derived from the two samplers. The lower correlation for PHE ($R = 0.62$) and FLT

($R = 0.57$) was most likely caused by the shorter integrative uptake in LDPE in comparison with SR. Although the two samplers were co-deployed for the same time period, the calculated $C_{w,LDPE}$ and $C_{w,SR}$ represent time-weighted average values over differing time periods. The good correlation of $C_{w,x}$ estimates obtained using the two passive samplers indicates that both samplers are suitable for the identification of concentration gradients and the assessment of compound trends in water column, e.g. along the Danube river.

However, the application of different models for calculation of $C_{w,LDPE}$ introduced various levels of systematic difference from the $C_{w,SR}$ estimates. Among the approaches tested, 'A' provided the best consistency of the results between the compared SR and LDPE samplers (Fig. 7) with the median $C_{w,SR}/C_{w,LDPE}$ ratio ranging from 0.7 for CHR to 2.2 for PHE. In contrast, the 'B' and 'C' options resulted in $C_{w,LDPE}$ values that were systematically lower than $C_{w,SR}$. In the case of model 'B', the median $C_{w,SR}/C_{w,LDPE}$ ratio ranged from 1.4 for CHR to 3.5 for PCB 28. In the case of approach 'C', the median $C_{w,SR}/C_{w,LDPE}$ ratio ranged from 2.2 for CHR to 4.4 for PCB 28.

To investigate the origin of differences in $C_{w,x}$ estimates, overall mass transfer coefficients $k_{o,x}$ of compounds accumulated in samplers were calculated as surface specific sampling rates ($k_{o,x} = R_{s,x}/A_x$). The required sampling rates were calculated from PRC release data using various models outlined in 2.4.1 The comparison of calculated $k_{o,x}$ values is shown in Fig. S15 in Supplementary information and in Table 2 (for results from model 'A' in 2.4.2, only). When models 'B' and 'C' were applied for calculation of $k_{o,LDPE}$, the calculated $k_{o,LDPE}/k_{o,SR}$ ratio is systematically higher than one (1.2 to 5.1) and in both models its value increases with increasing compound hydrophobicity or molar mass. Results of these two model calculations contradict the observed generally higher surface specific uptake in SR in comparison with LDPE (Fig. S8). The model 'A' calculates $k_{o,LDPE}$ for WBL controlled uptake to be equal to $k_{o,SR}$, and thus the $k_{o,LDPE}/k_{o,SR}$ ratio for all compounds excepting PHE is very close to unity (Fig. S15).

There are several factors that contribute to the systematic discrepancy between $k_{o,LDPE}$ values under WBL control obtained using models 'B' and 'C', and $k_{o,SR}$ values used in the model 'A'.

The model 'B' calculates $k_{o,LDPE}$, including resistances in WBL and membrane as a function of hydrophobicity, represented by log K_{ow} (Booij et al., 2003). It has been shown above that for this study, membrane resistance is negligible and calculation of the membrane resistance term is not relevant. Further, we argue that log K_{ow} is generally
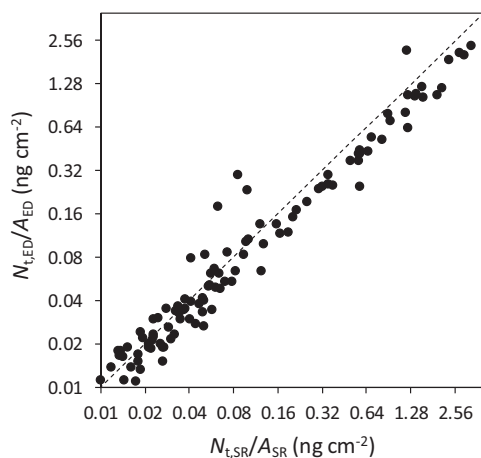

Fig. 6. Surface specific uptake of PAHs with log $K_{SR,w} > 4.5$and 4-nonylphenol (11 substances) in ED versus SR passive samplers deployed in DPS devices in 8 mobile and 2 stationary deployments. The dashed line indicates unity.
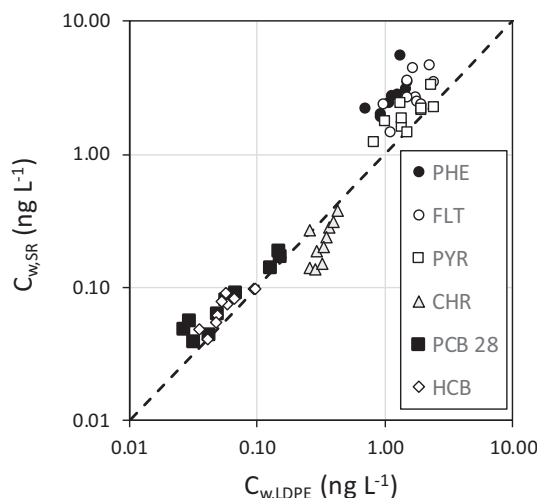

Fig. 7. Comparison of calculated free dissolved concentration in water $C_{w,x}$ (ng L^{-1}) of selected PAHs, and PCB 28 and HCB in LDPE and SR passive samplers deployed in DPS devices in 8 mobile and 2 stationary deployments. The dashed line represents equality of values. Sampling rates in LDPE were calculated using method 'A' outlined in Section 2.4.2.

not a good predictor neither for D_{LDPE} nor for $K_{LDPE,w}$ values required for $R_{s,LDPE}$ calculation.

The model 'C' derives $k_{o,LDPE}$ under WBL control as a weak function of molar mass, but it suffers from insufficient amount of available PRC data in the hydrophobicity range where partial dissipation (a single compound), highly relevant for an improved model accuracy (Booij and Smedes, 2010), would be expected.

Further, the accuracy of $k_{o,x}$ values largely depends on the quality of the $K_{x,w}$ values of the applied PRCs (Eqs. (3) and (6)). Booij and Smedes (2010) have shown that uncertainties in the $K_{x,w}$ values of the PRCs may result in an $R_{s,x}$ bias of about 0.3 log units. Since $k_{o,SR}$ calculation (model 'A') is derived from dissipation of more compounds than $k_{o,LDPE}$ (models 'B' and 'C'), the uncertainty of $k_{o,SR}$ is expected to be lower than that of $k_{o,LDPE}$. The accuracy of model fit largely depends on those PRCs that dissipate from samplers between 20 and 80%. In case of SR samplers, 2 to 5 PRCs fulfilled this criterion, whereas in LDPE samplers it was the case for only a single PRC. Furthermore, PCBs are generally considered to be more reliable PRCs than PAHs, mainly because of their better chemical stability. In view of the above mentioned uncertainties introduced by models 'B' and 'C', the model 'A' seems to be the best option for derivation of $C_{w,LDPE}$.

For PHE, sampling rate has no effect on the calculation of $C_{w,LDPE}$, since in all exposures, sampler has reached >90% partition equilibrium with water. This has been confirmed by an almost complete dissipation of d_{10}-PHE from LDPE in all exposures. For this compound, $C_{w,LDPE}$ can simply be calculated as $C_{w,LDPE} = C_{LPDE}/K_{LDPE,w}$. Thus, the accuracy of $C_{w,LDPE}$ estimate for PHE will strongly depend on the applied $K_{LDPE,w}$ value, whereas the accuracy of $C_{w,SR}$ depends mainly on the accuracy of the model that is used to derive the applied sampling rates (Lohmann et al., 2012). It has also been mentioned that the $C_{w,LDPE}$ and $C_{w,SR}$ values for PHE represent different periods of integrative sampling, and certain difference may reflect the temporal variability of PHE concentration in sampled water.

The results of this study as well as previous interlaboratory studies (Allan et al., 2009; Vrana et al., 2016), confirm a recommendation made by (Booij et al., 2017, 2016; Smedes et al., 2007) that standardization of $R_{s,x}$ estimation methods, improvement of analytical techniques, and the selection of high quality values for $K_{x,w}$ may greatly reduce interlaboratory variability of passive sampling results.

3.3. Derivation of sampling rates for ED samplers

Since a good correlation was obtained for the $N_{t,x}/A_x$ ratio of co-deployed SR and ED samplers, in situ cross-calibration was possible. The sampling rates of ED samplers $R_{s,ED}$ were estimated from sampling rates derived for SR samplers ($R_{s,SR}$), using the calculated overall median $F_{ED/SR}$ ratio of 0.83, and the surface areas of both samplers A_{ED}, A_{SR}:

$$R_{s,ED} = 0.83 \times \frac{A_{ED}}{A_{SR}} \times R_{s,SR} \quad (12)$$

The WBL controlled sampling rate estimate $R_{s,ED}$ obtained here should be from theory (Booij et al., 2007) a function of the compound's diffusion coefficient in water and can be estimated for any compound from its molar mass M using Eq. (5).

The applicability of the outlined approach is demonstrated for the measurement of atrazine in 8 stretches of the Danube river (Fig. 8). Atrazine was selected as a compound that was detectable in all spot water samples and passive samplers. In each of the 8 stretches, the estimate of $C_{w,ED}$ for atrazine lies within the range of concentration values measured in spot water samples collected during JDS3 within the river stretches (ICPDR International Commission for the Protection of the Danube River, n.d.).

When deriving free dissolved concentration from compound accumulation in ED, some limitations of this approach have to be considered. These include uncertainty of the Empore disk uptake capacity, since published values of Empore disk/water distribution coefficients are scarce and for polar dissociating compounds they will be affected by compounds pK_a value and water pH. The assumption of WBL controlled uptake may not be valid for all sampled compounds, especially those with low log $K_{x,w}$ values. Despite these limitations we believe that free dissolved concentrations estimated using the outlined cross-calibration approach provide values with lower uncertainty than those derived from the currently most widely applied adsorption passive sampler, the POCIS (Miège et al., 2015).

4. Conclusions and perspectives

The main DPS usage domain is a representative measurement of compound levels, averaged in time (TWA) and/or space. The DPS device presents a useful alternative approach to the conventional sampler deployment technique in cages in situations where integrative uptake of compounds accumulated under WBL control must be maximized.

We demonstrated the robustness of the DPS technique in stationary and mobile deployments in a large river. When DPS is used for sampling from a cruising ship, the device may be, alternatively to our deployment in a tank onboard a ship, directly immersed in the water column in front of the ship. However, such deployment may be difficult in practice because the device may be easily damaged or it may present an undesired obstacle to ship navigation.
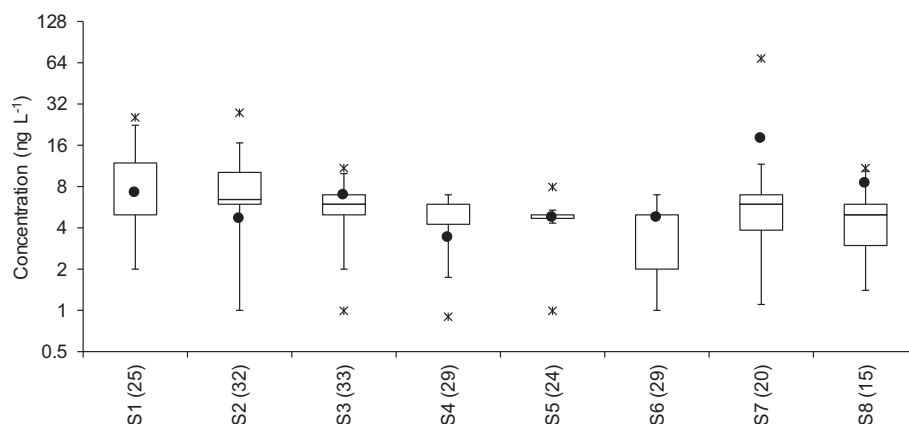

Fig. 8. Comparison of dissolved concentration of atrazine in water $C_{w,ED}$ (µg L^{-1}) estimated from ED deployed in DPS devices in mobile exposures along 8 Danube stretches (S1–S8; black dots) with concentrations in spot water samples collected during JDS3 survey within each stretch (box plots). The box in the plot comprises data between 25th and 75th percentile (interquartile range; IQR) with the median of the data shown by the horizontal line inside the box. The ends of whiskers represent the range within 1.5 IQR of the lower and upper quartile, respectively. Extreme values found in spot samples are labeled by asterisks. The numbers in brackets on x-axis denote the numbers of spot samples analysed within each stretch.

Aqueous concentrations of PAHs, PCBs and HCB derived from DPS did not differ from those obtained using conventional caged passive sampling. A good agreement was also found between aqueous concentrations derived from DPS devices deployed from a cruising ship and those deployed from river shore. The DPS sampled up to five times faster in comparison with a caged passive sampler deployed in a streaming river water. This feature presents a great advantage for integrative sampling of large equivalent volumes of water in a short time, when polymers with a high compound uptake capacity ($K_{x,w} \times m_x$) are used. We expect even higher differences in sampling rates between DPS and caged samplers when a comparison is performed under quiescent flow conditions.

The co-deployment of three passive samplers made of different sorbents in the DPS device, namely SR, LDPE and ED, allowed to extend the range of sampled compounds from non-polar to more hydrophilic ones. For all three co-deployed samplers we showed equivalent surface specific uptake for compounds that were sampled integratively during the entire exposure period. This indicates that mass transfer was dominantly WBL controlled and in such case the mass transfer coefficient is equivalent for all applied sampler types. The differences in calculated aqueous concentrations between LDPE and SR sampler were mainly associated with different applied uptake models. For hydrophobic compounds, aqueous concentrations derived from SR and LDPE samplers uptake agreed well when mass transfer coefficients derived for SR samplers were applied to the LDPE samplers.

The equivalent surface specific compound uptake provided a good basis for a cross-calibration between the samplers and allowed derivation of aqueous concentrations also from compound uptake in SDB-RPS Empore™ disks, for which the performance reference compound approach is not applicable. We showed that aqueous atrazine concentrations derived from uptake by ED were in good agreement with concentration obtained by spot sampling.

Besides mobile sampling in rivers or along lake or sea transects, application of the DPS can be beneficial in scenarios with only short practicable deployment times or in lakes or water bodies with low natural flow velocities, in cold/arctic conditions, everywhere where low sampling rates are expected with caged passive samplers. The practical application of DPS is somewhat limited by the need of external power source for driving the pump. Since strong water currents are created by operation of the DPS device, it is not particularly suitable for investigation of depth chemical stratification in stagnant water bodies. During deployment sampler exposure to sunlight is minimised, and this effectively prevents photo degradation of compounds. The strong current inside the exposure chamber minimises production of biofouling and samplers do not require extensive cleaning even after long deployments.

List of terms and abbreviations

A_x sampler × surface area in contact with water

Caged passive sampler   a passive sampler deployed in a cage made of perforated stainless steel sheet; It was deployed stationary in the Danube downstream Bratislava (see Table 1).

DPS   Dynamic Passive Sampling device; a novel water sampling device which forces water along the surface of sorbent sheets in a stainless steel flow-through chamber. Water passes through the chamber at a high flow rate assisted by a pump. This leads to a high turbulence close to the sorbent surface, and therefore to higher sampling rates when compared to conventional caged passive samplers.

D_x diffusion coefficient of a compound in the phase x

DEQ_x the degree of equilibrium that the compound attained during sampler x exposure

δ_x thickness of phase x

ED   Empore disk

$F_{ED/SR}$ the ratio of surface specific compound uptake in ED and SR samplers

GPC   gel permeation chromatography

HCB   hexachlorobenzene

$k_{o,x}$ overall mass transfer coefficient

k_w mass transfer coefficient in the water boundary layer

k_x mass transfer coefficient in the polymer x

K_{ow} octanol-water partition coefficient

$K_{x,w}$ polymer x–water partition coefficient

LDPE   low density polyethylene

LOQ   limit of quantification

m_x sampler mass

M molar mass of a compound

Mobile deployment   deployment of a passive sampler from a moving object, e.g. from a ship

$N_{t,x}$ amount of a compound accumulated in the sampler x after exposure time t

OCPs   organochlorinated pesticides

PAHs   polycyclic aromatic hydrocarbons

PCBs   polychlorinated biphenyls

PRC   performance reference compound(s).

RIS   recovery internal standard

$R_{s,x}$ sampling rate; the substance specific volume of water extracted per unit of time

$^{300}R_{s,x}$ sampling rate for a compound with molar mass $M = 300$ g mol^{-1}

Spot water sample   samples of whole water that were collected using bottles from the expedition ship at 63 sites in the 8 Danube stretches covered by passive sampling. Spot samples reflect water quality only at the point in time that the sample was collected.

Stationary deployment   deployment of a passive sampler at a fixed place.

SR   silicone rubber

WBL   water boundary layer

Appendix A. Supplementary data

Supplementary data associated with this article can be found in the online version, at https://doi.org/10.1016/j.scitotenv.2018.03.242. These data include the Google map of the most important areas described in this article.

References

Allan, I.J., Booij, K., Paschke, A., Vrana, B., Mills, G.A., Greenwood, R., 2009. Field performance of seven passive sampling devices for monitoring of hydrophobic substances. Environ. Sci. Technol. 43, 5383–5390.

Allan, I.J., Nilsson, H.C., Tjensvoll, I., Bradshaw, C., Næs, K., 2011. Mobile passive samplers: concept for a novel mode of exposure. Environ. Pollut. 159:2393–2397. https://doi.org/10.1016/j.envpol.2011.06.039.

Allan, I.J., Harman, C., Ranneklev, S.B., Thomas, K.V., Grung, M., 2013. Passive sampling for target and nontarget analyses of moderately polar and nonpolar substances in water. Environ. Toxicol. Chem. 32:1718–1726. https://doi.org/10.1002/etc.2260.

Booij, K., Smedes, F., 2010. An improved method for estimating in situ sampling rates of nonpolar passive samplers. Environ. Sci. Technol. 44, 6789–6794.

Booij, K., Hofmans, H.E., Fischer, C.V., van Weerlee, E.M., 2003. Temperature-dependent uptake rates of nonpolar organic compounds by semipermeable membrane devices and low-density polyethylene membranes. Environ. Sci. Technol. 37, 361–366.

Booij, K., Vrana, B., Huckins, J.N., 2007. Theory, modelling and calibration of passive samplers used in water monitoring. In: Greenwood, R., Mills, G., Vrana, B. (Eds.), Comprehensive Analytical Chemistry 48. Passive Sampling Techniques in Environmental Monitoring. Elsevier, Amsterdam:pp. 141–169 https://doi.org/10.1016/S0166-526X(06)48007-7.

Booij, K., Robinson, C.D., Burgess, R.M., Mayer, P., Roberts, C.A., Ahrens, L., Allan, I.J., Brant, J., Jones, L., Kraus, U.R., Larsen, M.M., Lepom, P., Petersen, J., Pröfrock, D., Roose, P., Schäfer, S., Smedes, F., Tixier, C., Vorkamp, K., Whitehouse, P., 2016. Passive sampling in regulatory chemical monitoring of nonpolar organic compounds in the aquatic environment. Environ. Sci. Technol. 50, 3–17. doi:https://doi.org/10.1021/acs.est.5b04050.l

Booij, K., Smedes, F., Crum, S., 2017. Laboratory performance study for passive sampling of nonpolar chemicals in water. Environ. Toxicol. Chem. 36:1156–1161. https://doi.org/10.1002/etc.3657.

Deutsch, K., Sengl, M., 2015. Priority and other organic substances. In: Liška, I., Wagner, F., Sengl, M., Deutsch, K., Slobodník, J. (Eds.), Joint Danube Survey 3. A Comprehensive Analysis of Danube Water Quality. ICPDR – International Commission for the Protection of the Danube River, Vienna, pp. 211–222.

Estoppey, N., Schopfer, A., Omlin, J., Esseiva, P., Vermeirssen, E.L.M., Delémont, O., de Alencastro, L.F., 2014. Effect of water velocity on the uptake of polychlorinated biphenyls (PCBs) by silicone rubber (SR) and low-density polyethylene (LDPE) passive samplers: an assessment of the efficiency of performance reference compounds (PRCs) in river-like flow condition. Sci. Total Environ. 499:319–326. https://doi.org/10.1016/j.scitotenv.2014.08.047.

EU, 2000. Directive 2000/60/EC of the European parliament and of the council of 23 October 2000 establishing a framework for community action in the field of water policy. Off. J. Eur. Union L327, 1–72.

EU, 2013. Directive 2013/39/EU of the European Parlament and of the Council of 12 August 2013 amending directives 2000/60/EC and 2008/105/EC as regards priority substances in the field of water policy. Off. J. Eur. Union L226, 1–17.

ICPDR International Commission for the Protection of the Danube River, n.d. Danube River Basin Water Quality Database [WWW Document]. URL http://www.icpdr.org/wq-db/ (accessed 2.3.18).

Levich, V.G., 1962. Convective diffusion in liquids. Physicochemical Hydrodynamics. Prentice-Hall, Englewood Cliffs, N.J., pp. 139–183.

Li, H., Vermeirssen, E.L., Helm, P.A., Metcalfe, C.D., 2010. Controlled field evaluation of water flow rate effects on sampling polar organic compounds using polar organic chemical integrative samplers. Environ. Toxicol. Chem. 29, 2461–2469.

Liška, I., Wagner, F., Sengl, M., Deutsch, K., Slobodník, J., 2015. A comprehensive analysis of Danube water quality. Joint Danube Survey 3. ICPDR – International Commission for the Protection of the Danube River, Vienna.

Lohmann, R., Booij, K., Smedes, F., Vrana, B., 2012. Use of passive sampling devices for monitoring and compliance checking of POP concentrations in water. Environ. Sci. Pollut. Res. Int. 19:1885–1895. https://doi.org/10.1007/s11356-012-0748-9.

Miège, C., Mazzella, N., Allan, I., Dulio, V., Smedes, F., Tixier, C., Vermeirssen, E., Brant, J., O'Toole, S., Budzinski, H., Ghestem, J.-P., Staub, P.-F., Lardy-Fontan, S., Gonzalez, J.-L., Coquery, M., Vrana, B., 2015. Position paper on passive sampling techniques for the monitoring of contaminants in the aquatic environment - achievements to date and perspectives. Trends Environ. Anal. Chem. 8:20–26. https://doi.org/10.1016/j.teac.2015.07.001.

Petersen, W., 2014. FerryBox systems: state-of-the-art in Europe and future development. J. Mar. Syst. 140:4–12. https://doi.org/10.1016/j.jmarsys.2014.07.003.

Petersen, J., Pröfrock, D., Paschke, A., Broekaert, J.A.C., Prange, A., 2016. Development and field test of a mobile continuous flow system utilizing Chemcatcher for monitoring of rare earth elements in marine environments. Environ. Sci. Water Res. Technol. 2: 146–153. https://doi.org/10.1039/C5EW00126A.

Qin, Z., Bragg, L., Ouyang, G., Niri, V.H., Pawliszyn, J., 2009. Solid-phase microextraction under controlled agitation conditions for rapid on-site sampling of organic pollutants in water. J. Chromatogr. A 1216:6979–6985. https://doi.org/10.1016/j.chroma.2009.08.052.

Reichenberg, F., Mayer, P., 2006. Two complementary sides of bioavailability: accessibility and chemical activity of organic contaminants in sediments and soils. Environ. Toxicol. Chem. 25, 1239–1245.

Rusina, T., Smedes, F., Klanova, J., Booij, K., Holoubek, I., 2007. Polymer selection for passive sampling: a comparison of critical properties. Chemosphere 68, 1344–1351.

Rusina, T., Smedes, F., Klanova, J., 2010a. Diffusion coefficients of polychlorinated biphenyls and polycyclic aromatic hydrocarbons in polydimethylsiloxane and low-density polyethylene polymers. J. Appl. Polym. Sci. 116, 1803–1810.

Rusina, T., Smedes, F., Koblizkova, M., Klanova, J., 2010b. Calibration of silicone rubber passive samplers: experimental and modeled relations between sampling rate and compound properties. Environ. Sci. Technol. 44, 362–367.

Salaun, P., Buffle, J., 2004. Integrated microanalytical system coupling permeation liquid membrane and voltammetry for trace metal speciation. Theory and applications. Anal. Chem. 76, 31–39.

Shaw, M., Eaglesham, G., Mueller, J.F., 2009. Uptake and release of polar compounds in SDB-RPS Empore™ disks; implications for their use as passive samplers. Chemosphere 75:1–7. https://doi.org/10.1016/j.chemosphere.2008.11.072.

Smedes, F., Booij, K., 2012. Guidelines for Passive Sampling of Hydrophobic Contaminants in Water Using Silicone Rubber Samplers. [WWW Document]. URL http://www.rs.passivesampling.net/PSguidanceTimes52.pdf.

Smedes, F., van der Zande, T., Roose, P., Davies, I.M., 2007. ICES passive sampling trial survey for water and sediment (PSTS) 2006–2007. Part 3: preliminary interpretation of field data. [WWW Document]. URL http://www.ices.dk/sites/pub/CMDoccuments/CM-2007/J/J0407.pdf, Accessed date: 2 February 2018.

Smedes, F., Geertsma, R.W., Van Der Zande, T., Booij, K., 2009. Polymer-water partition coefficients of hydrophobic compounds for passive sampling: application of cosolvent models for validation. Environ. Sci. Technol. 43, 7047–7054.

Ter Laak, T.L., Busser, F.J.M., Hermens, J.L.M., 2008. Poly(Dimethylsiloxane) as passive sampler material for hydrophobic chemicals: effect of chemical properties and sampler characteristics on partitioning and equilibration times. Anal. Chem. 80, 3859–3866.

Umlauf, G., Giulio, M., Helle, S., 2015. Spatial and temporal trends of Dioxins, PCBs and BDE-209 in suspended particulate matter and fish – JDS3 versus JDS2. In: Liška, I., Wagner, F., Sengl, M., Deutsch, K., Slobodník, J. (Eds.), Joint Danube Survey 3. A Comprehensive Analysis of Danube Water Quality. ICPDR – International Commission for the Protection of the Danube River, Vienna, pp. 249–259.

Vermeirssen, E.L.M., Bramaz, N., Hollender, J., Singer, H., Escher, B.I., 2009. Passive sampling combined with ecotoxicological and chemical analysis of pharmaceuticals and biocides - evaluation of three Chemcatcher configurations. Water Res. 43:903–914. https://doi.org/10.1016/j.watres.2008.11.026.

Vrana, B., Schüürmann, G., 2002. Calibrating the uptake kinetics of semipermeable membrane devices in water: impact of hydrodynamics. Environ. Sci. Technol. 36, 290–296.

Vrana, B., Allan, I.J., Greenwood, R., Mills, G.A., Dominiak, E., Svensson, K., Knutsson, J., Morrison, G., 2005. Passive sampling techniques for monitoring pollutants in water. TrAC - Trends Anal. Chem. 24, 845–868.

Vrana, B., Klučárová, V., Benická, E., Abou-Mrad, N., Amdany, R., Horáková, S., Draxler, A., Humer, F., Gans, O., 2014. Passive sampling: an effective method for monitoring seasonal and spatial variability of dissolved hydrophobic organic contaminants and metals in the Danube river. Environ. Pollut. 184, 101–112.

Vrana, B., Smedes, F., Prokeš, R., Loos, R., Mazzella, N., Miege, C., Budzinski, H., Vermeirssen, E., Ocelka, T., Gravell, A., Kaserzon, S., 2016. An interlaboratory study on passive sampling of emerging water pollutants. TrAC Trends Anal. Chem. 76: 153–165. https://doi.org/10.1016/j.trac.2015.10.013.